

**Catalyst Displacement Assay: A Supramolecular Approach for Design of Smart Latent  
Catalysts for Pollutant Monitoring and Removal**

**Supporting information**

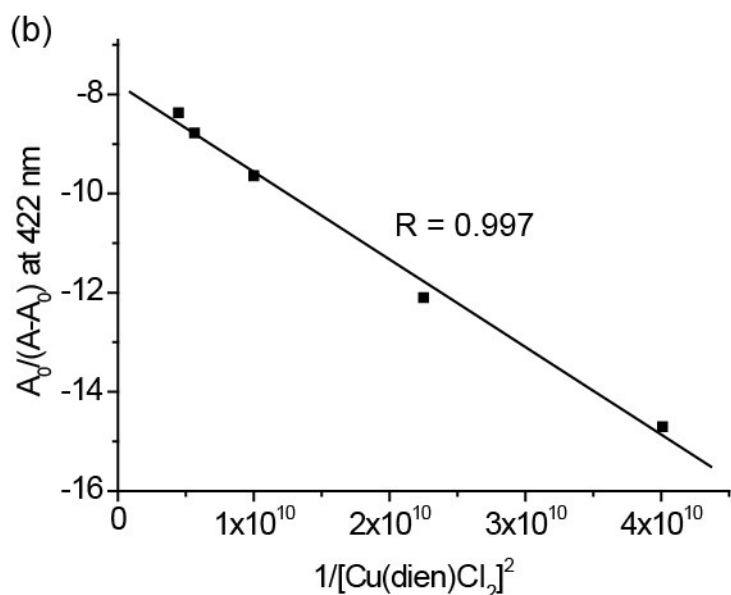
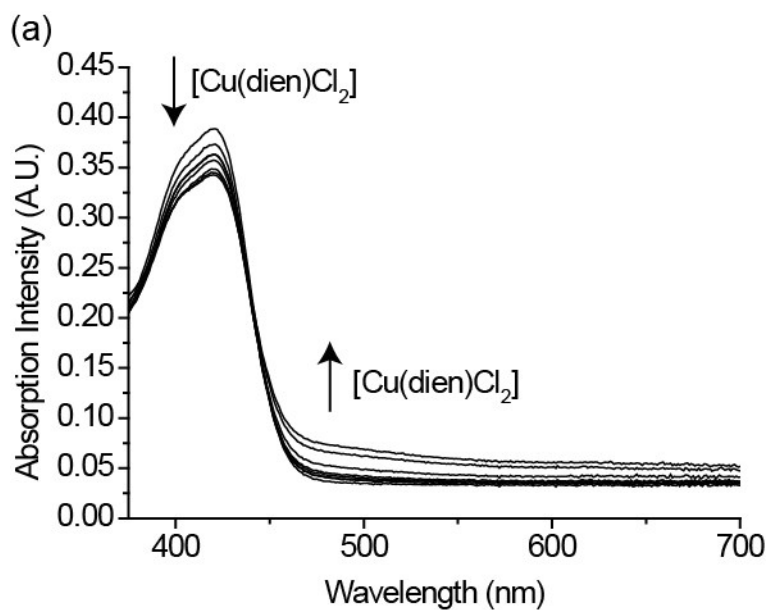
Cheuk-Fai Chow,<sup>\*[a]</sup> Pui-Yu Ho,<sup>[b]</sup> Cheng-Bin Gong,<sup>\*[a]</sup> Yu-Jing Lu,<sup>[c]</sup> Qian Tang<sup>[a]</sup> and  
Wing-Leung Wong<sup>\*[b]</sup>

<sup>a</sup>Department of Science and Environmental Studies, The Education University of Hong Kong,  
10 Lo Ping Road, Tai Po Hong Kong SAR, China and College of Chemistry and Chemical  
Engineering, Southwest University, Chong Qing, China

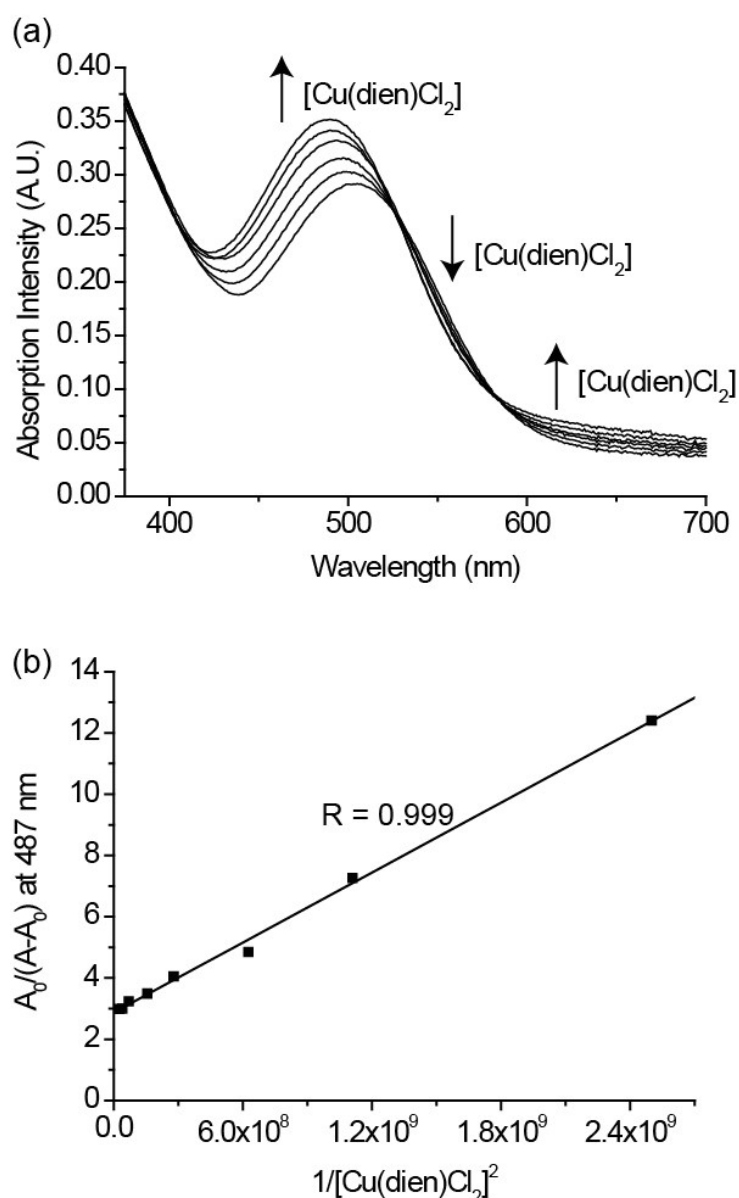
<sup>b</sup>Centre for Education in Environmental Sustainability, The Education University of Hong  
Kong, 10 Lo Ping Road, Tai Po, Hong Kong SAR, China.

<sup>c</sup>Institute of Natural Medicine and Green Chemistry, School of Chemical Engineering and  
Light Industry, Guangdong University of Technology, Guangzhou 510006, P.R. China.

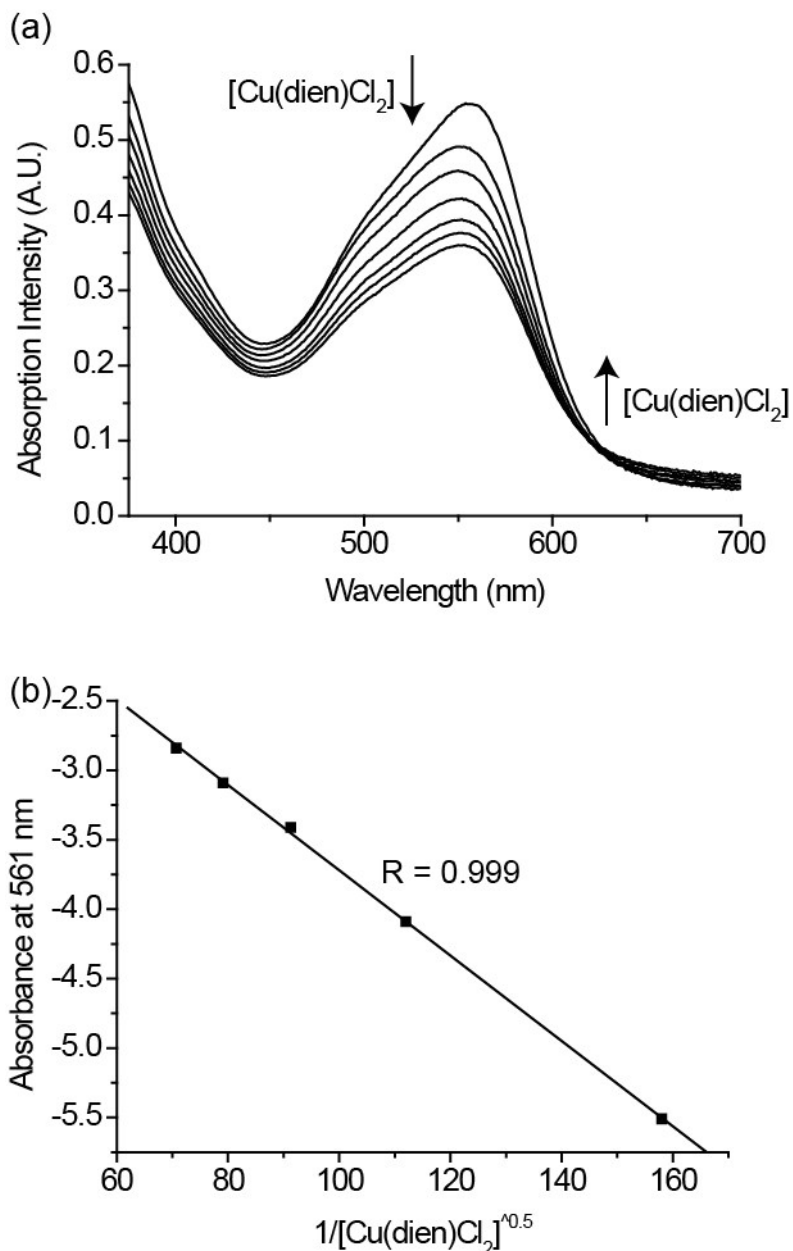
E-mail: cfchow@ied.edu.hk; Fax: (+852) 29487676; Tel: (+852) 29487671



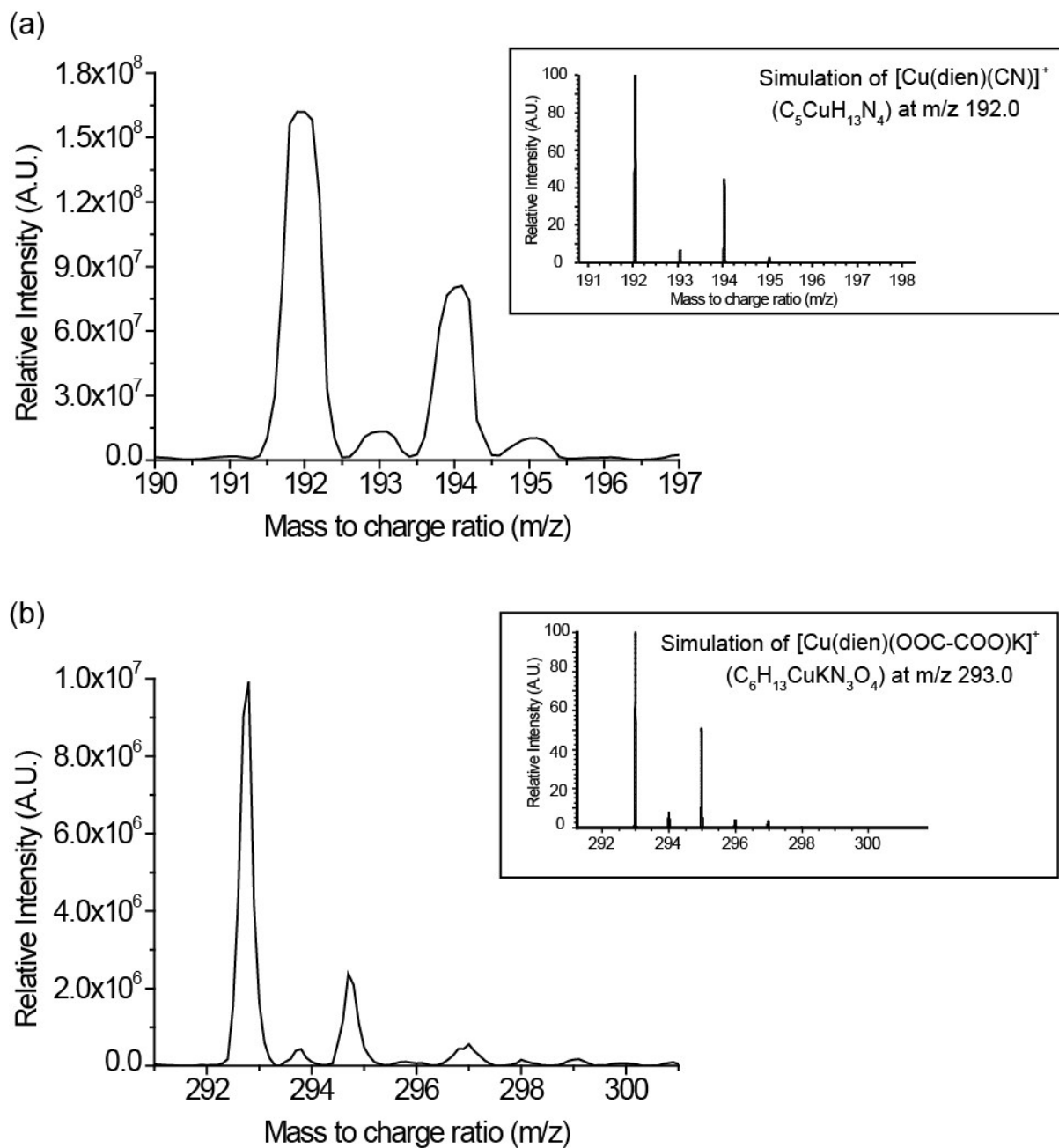
**SI.Figure 1.** (a) Spectroscopic titrations of  $K_4[Fe^{II}(CN)_6]$  ( $3.3 \times 10^{-4}$  M) by  $Cu^{II}(dien)Cl_2$  (0 to  $2 \times 10^{-5}$  M) (b) The slope and y-intercept are  $-1.77 \times 10^{-10}$  M and  $-7.79$  respectively of the best fitted  $A_0/(A-A_0)$  versus  $1/\{[Cu^{II}(dien)Cl_2]\}^2$  plot with  $\log K = 5.32 \pm 0.008$  at 422 nm. From fitting the curve with the ratio 1:2 Benesi-Hildebrand equation, the solvated form of the complex is deduced as 1:2 ratio of  $[Fe^{II}:Cu^{II}]$ . All the titrations were performed in HEPES buffer at pH 7.4 at 298 K.



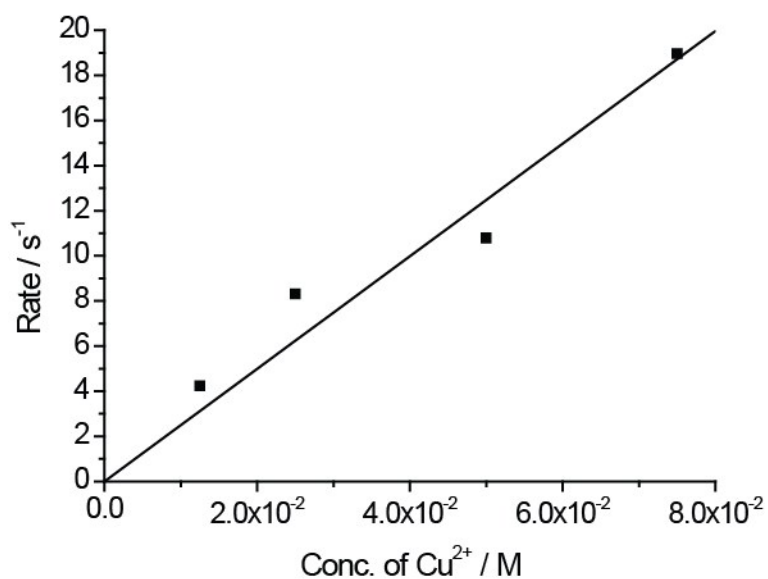
**SI.Figure 2.** (a) Spectroscopic titrations of  $K_2[Fe^{II}('Bubpy)(CN)_4]$  ( $5 \times 10^{-5}$  M) by  $Cu^{II}(dien)Cl_2$  (0 to  $2 \times 10^{-4}$  M) (b) The slope and y-intercept are  $3.80 \times 10^{-9}$  M and 2.88 respectively of the best fitted  $A_0/(A-A_0)$  versus  $1/\{[Cu^{II}(dien)Cl_2]\}^2$  plot with  $\log K = 4.44 \pm 0.001$  at 487 nm. From fitting the curve with the ratio 1:2 Benesi-Hildebrand equation, the solvated form of the complex is deduced as 1:2 ratio of  $[Fe^{II}:Cu^{II}]$ . All the titrations were performed in aqueous DMF (1:1 v/v) (1.50 mL of aqueous HEPES buffer at pH 7.4 + 1.50 mL of DMF) at 298 K.



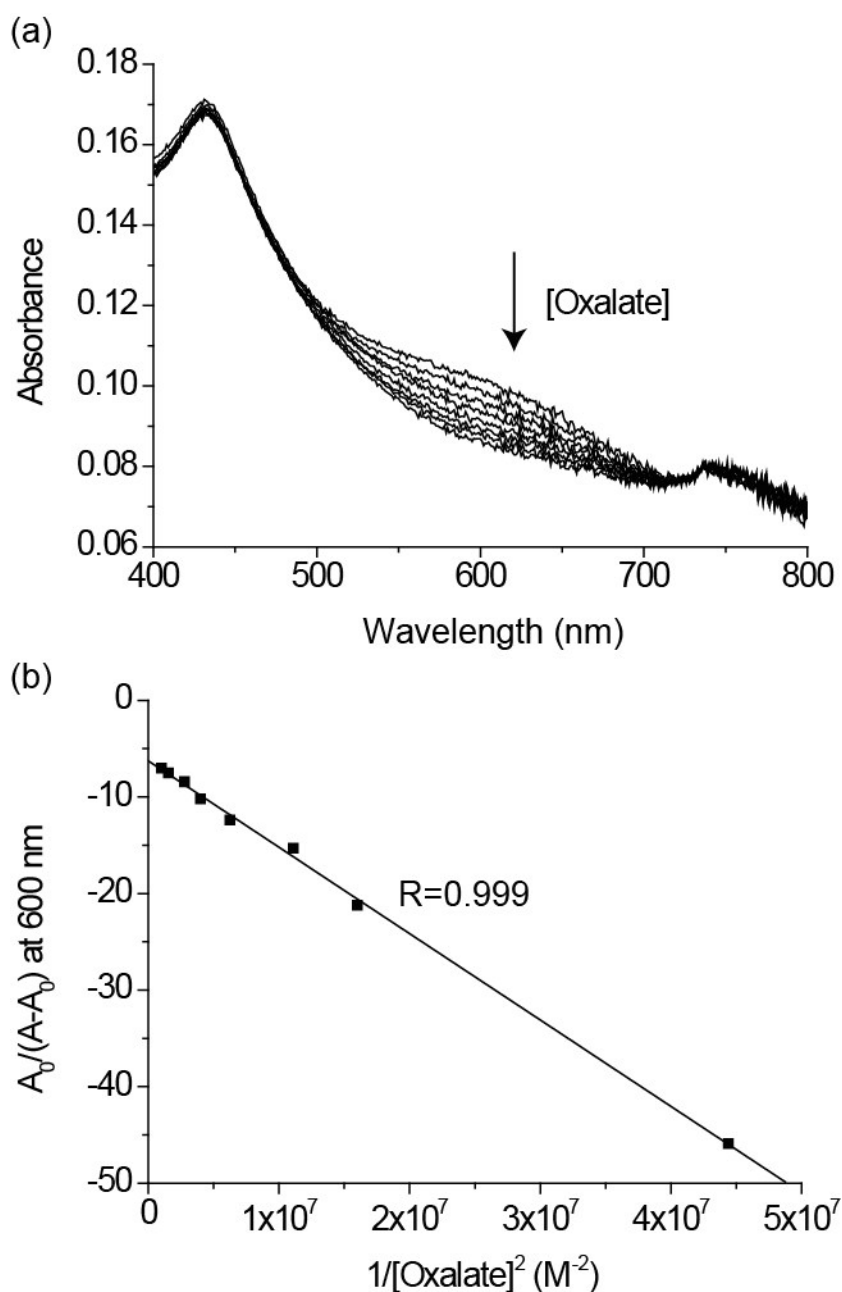
**SI.Figure 3.** (a) Spectroscopic titrations of  $\text{Fe}^{\text{II}}(\text{tBubpy})_2(\text{CN})_2$  ( $5 \times 10^{-5}$  M) by  $\text{Cu}^{\text{II}}(\text{dien})\text{Cl}_2$  (0 to  $1 \times 10^{-4}$  M) (b) The slope and y-intercept are  $-3.07 \times 10^{-2}$  M and  $6.51 \times 10^{-1}$  respectively of the best fitted  $A_0/(A-A_0)$  versus  $1/\{[\text{Cu}^{\text{II}}(\text{dien})\text{Cl}_2]^{0.5}\}$  plot with  $\log K = 2.65 \pm 0.001$  at 561 nm. From fitting the curve with the ratio 0.5:1 Benesi-Hildebrand equation, the solvated form of the complex is deduced as 0.5:1 ratio of  $[\text{Fe}^{\text{II}}:\text{Cu}^{\text{II}}]$ . All the titrations were performed in aqueous DMF (1:1 v/v) (1.50 mL of aqueous HEPES buffer at pH 7.4 + 1.50 mL of DMF) at 298 K.



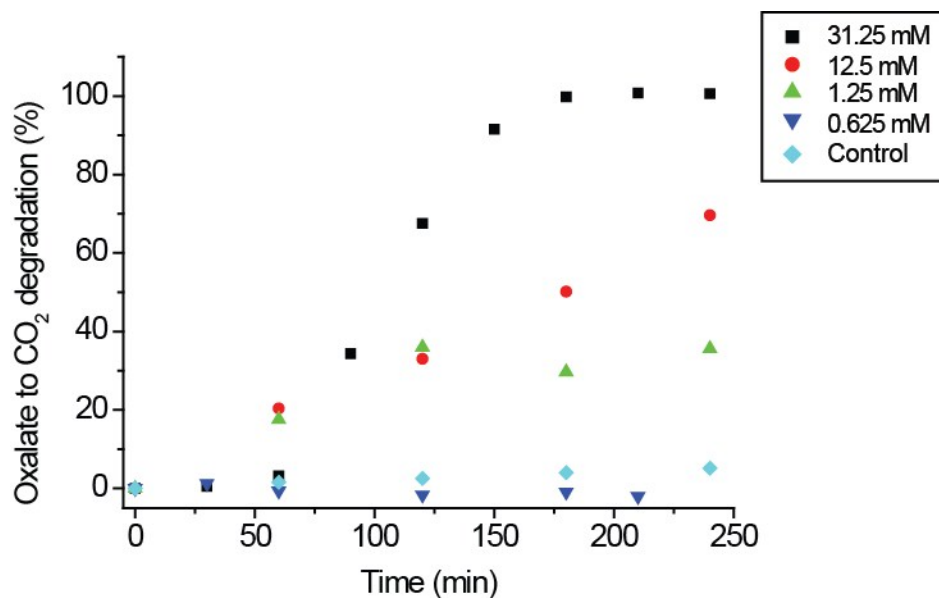
**SI.Figure 4.** Electrospray mass spectra of (a) “complex 1 / 2 or 3-cyanide-mixture” and (*inset*) the simulation of  $[\text{Cu}^{\text{II}}(\text{dien})(\text{CN})]^+$  ( $m/z$  192.0); and (b) “complex 1/ 2 or 3-oxalate-mixture” and (*inset*) the simulation of  $[\text{Cu}^{\text{II}}(\text{dien})(\text{OOC-COO})(\text{K})]^+$  ( $m/z$  293.0). The mass spectra were performed in aqueous methanol.



**SI.Figure 5.** Kinetic plot of apparent association rate constant  $k_{obs}$  ( $s^{-1}$ ) versus  $Cu^{2+}$  concentration. The rate constant value was calculated from the slope ( $249.5 M^{-1}s^{-1}$ ) of the curve ( $y = mx$ ). All the  $k_{obs}$  data were retrieved from Sarla, M.; Pandit, M.; Tyagi, D. K.; Kapoor, J. C. *J. Hazard. Mater.* **2004**, *B116*, 49-56.

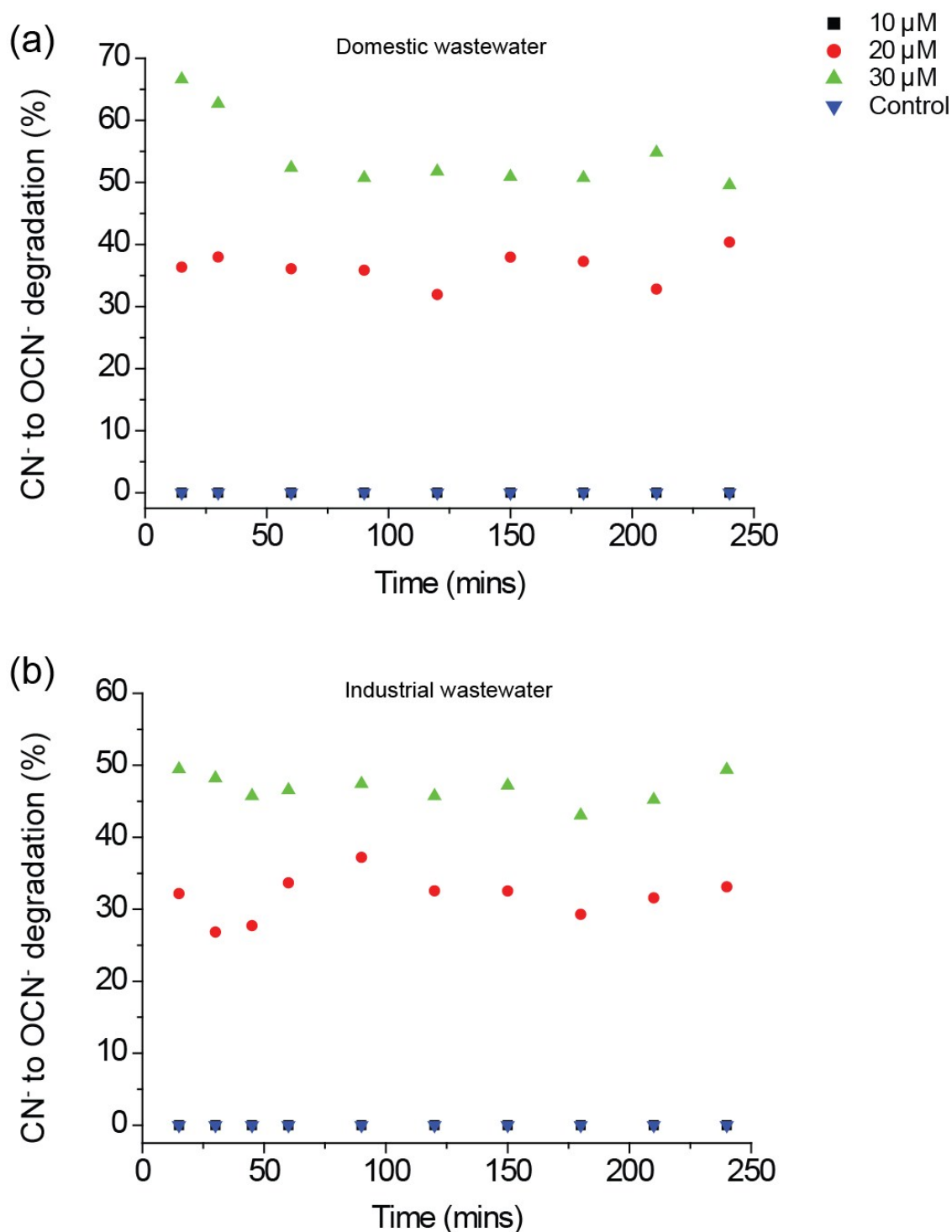


**SI.Figure 6.** (a) UV-vis spectroscopic titrations of  $\text{Cu}^{\text{II}}(\text{dien})\text{Cl}_2$  ( $5 \times 10^{-4}$  M) with oxalate (0 to  $1 \times 10^{-3}$  M). (b) The slope and y-intercept are  $-8.95 \times 10^{-7}$  M and  $-6.25 \times 10^{-1}$  respectively of the best fitted  $A_0/(A-A_0)$  versus  $1/[\text{oxalate}]^2$  plot with  $\log K = 6.84 \pm 0.002$  at 600 nm. All titrations were carried out in aqueous phosphate buffer pH 4 at 298 K.



**SI.Figure 7.** Formation of CO<sub>2</sub> with respect to different initial concentration of oxalate in the presence of complex **1** ( $6.25 \times 10^{-4}$  M) against time. The formation of CO<sub>2</sub> in the absence of catalyst (●). All the experiments were performed with H<sub>2</sub>O<sub>2</sub> (0.4 M) and pH 3 at room temperature and UV-vis irradiation under an open atmosphere.





**SI. Figure 8.** Conversion of cyanide to cyanate in real sample of (a) domestic wastewater (level I, untreated) and (b) industrial wastewater by **3** ( $2.0 \times 10^{-4}\text{M}$ ) in the presence of  $\text{H}_2\text{O}_2$  ( $6.53 \times 10^{-4}\text{M}$ ) and spiked with (■) 10  $\mu\text{M}$ , (●) 20  $\mu\text{M}$  and (▲) 30  $\mu\text{M}$  of cyanide. Control experiments (▼) were run in the absence of **3**, but in presence of  $\text{H}_2\text{O}_2$  ( $6.53 \times 10^{-4}\text{M}$ ) and spiked with 10  $\mu\text{M}$  cyanide.

**SI.Figure 9.** Full range ESI-MS spectra of complexes **1- 3**. All the experiments were conducted in DI water/methanol.

